DISCLAIMER

This report was prepared as an account of work sponsored by an agency of the United States Government. Neither the United States Government nor any agency thereof, nor any of their employees, makes any warranty, express or implied, or assumes any legal liability or responsibility for the accuracy, completeness, or usefulness of any information, apparatus, product, or process disclosed, or represents that its use would not infringe privately owned rights. Reference herein to any specific commercial product, process, or service by trade name, trademark, manufacturer, or otherwise does not necessarily constitute or imply its endorsement, recommendation, or favoring by the United States Government or any agency thereof. The views and opinions of authors expressed herein do not necessarily state or reflect those of the United States Government or any agency thereof. Reference herein to any social initiative (including but not limited to Diversity, Equity, and Inclusion (DEI); Community Benefits Plans (CBP); Justice 40; etc.) is made by the Author independent of any current requirement by the United States Government and does not constitute or imply endorsement, recommendation, or support by the United States Government or any agency thereof.

BNL-229489-2026-TECH
EIC-ADD-TN-159

Thermal Compton Scattering of Electron Beams on Blackbody Photons: A Monte Carlo Event Generator for Multi-Turn Tracking at the Electron-Ion Collider

A. Natochii

February 2026

Electron-Ion Collider

Brookhaven National Laboratory

U.S. Department of Energy

USDOE Office of Science (SC), Nuclear Physics (NP)

DISCLAIMER

Thermal Compton Scattering of Electron Beams on Blackbody Photons: A Monte Carlo Event Generator for Multi-Turn Tracking at the Electron-Ion Collider

Andrii Natochii*
Brookhaven National Laboratory, Upton, New York 11973, USA
(Dated: February 25, 2026)

Compton scattering of ultra-relativistic electrons on thermal (blackbody) photons is typically a subdominant process in electron storage rings, but at sufficiently high electron energy and low residual gas pressure it can become competitive with beam-gas scattering and contribute to distributed losses and backgrounds. We present a self-contained Monte Carlo event generator for thermal Compton scattering designed for integration into multi-turn tracking workflows. The implementation follows H. Burkhardt's proposal method: trial scattering angles are sampled from the Thomson differential cross section and accepted/rejected using the Klein-Nishina to Thomson ratio, yielding the correct Compton spectrum while retaining simple absolute-rate normalization. Thermal photon energies are sampled from the blackbody photon-number spectrum via an exact mixture representation. Each accepted event is assigned an absolute rate weight in Hz derived from beam current, blackbody photon density, the Thomson cross section, and section length, enabling direct computation of scattering and loss rates from tracked events. Using the Electron-Ion Collider (EIC) electron storage ring (ESR) lattice and multi-turn tracking, we compute ring loss maps, loss timing distributions, and beam lifetimes for $E = 5$, 10, and 18 GeV at $T = 300$ K and nominal EIC beam currents. The results show that thermal-radiation losses are predominantly localized at collimators and the final focusing system and produce a distributed loss pattern around the ring. At 18 GeV, thermal-radiation yields a shorter lifetime (~ 120 h) than the beam-gas+Touschek (~ 200 h) for the studied configuration. The generator and validation scripts are intended for public release to support reproducibility and reuse by the accelerator community.

I. INTRODUCTION

High-energy electron storage rings are subject to several beam-loss mechanisms, which under standard operating conditions are typically dominated by beam-gas interactions and Touschek scattering. At sufficiently high electron energies and low residual-gas pressure, Compton scattering on thermal (blackbody) photons can become competitive and produce losses[1] distributed around the ring. Early analytic studies [1] show that this process can limit the beam lifetime for momentum acceptances at the $\mathcal{O}(1\%)$ level, with a strong dependence on beam energy and aperture acceptance.

The Electron-Ion Collider (EIC) [2] electron storage ring (ESR) will provide a representative case where several scattering mechanisms contribute to the overall loss budget. The ESR loss studies presented below indicate that Bethe-Heitler bremsstrahlung at the interaction point (IP) and thermal-radiation Compton scattering can generate distributed losses and, at high electron energy, yield lifetimes shorter than those obtained in earlier beam-gas and Touschek-only evaluations [3].

In addition to physics motivation, a practical motivation is software: thermal Compton scattering needs (i) correct relativistic kinematics across multiple frames, (ii) correct Klein-Nishina (KN) distributions, (iii) numerically stable generation of rare tail events that exceed ring acceptance, and (iv) correct absolute normalization so tracked losses can be converted into lifetimes and heat-load-relevant rates. Many tracking workflows do not include a ready-to-use, validated thermal Compton generator with absolute rate weights.

This paper contributes:

- a standalone, publicly releasable thermal Compton event generator suitable for embedding into multi-turn tracking codes,
- an efficient and accurate thermal photon energy sampler for the blackbody photon-number distribution,
- absolute event-rate normalization in Hz consistent with beam current and photon number density, and
- ESR loss maps, timing distributions, and lifetime estimates for design energies and beam currents.

Although the Monte Carlo approach for thermal Compton scattering was described in 1993 [4] and implemented in the THEGEN framework (FORTRAN) and can be obtained from H. Burkhardt (CERN), providing a clear and influential foundation for this topic, many present-day accelerator studies benefit from having a compact, tracking-oriented implementation that can be readily integrated into modern simulation chains. The original publication lays out the essential method and sampling strategy. In this work, we present an independent implementation following the algorithmic description in Ref. [4], adapted to the EIC use case and packaged as a small, self-contained module intended for public release. The implementation retains the key physics

* Contact author: natochii@bnl.gov
[1] Particles are counted as lost when they intersect the machine aperture (i.e., vacuum beam pipe or collimator surfaces).

ingredients such as Thomson-angle proposal sampling with KN acceptance, explicit Lorentz/rotation kinematics, and absolute rate normalization, while making use of modern numerical utilities (e.g., stable mixture sampling and reproducible random-number generator control) and providing validation and plotting scripts to facilitate independent verification and long-term reuse.

The paper is structured as follows. Section II summarizes the EIC collider and detector context. Section III describes beam loss mechanisms relevant to this study and positions thermal Compton among them. Section IV presents the physics model and event-generation method. Section V describes the multi-turn tracking integration and simulation assumptions. Section VI presents results: loss maps (ring and IR), timing distributions, and lifetimes. Section VII outlines validation tests and public software release contents. Section VIII provides discussion and limitations. Section IX summarizes conclusions and future work.

II. COLLIDER AND DETECTOR OVERVIEW

A. Collider Design

The EIC will be built in the existing 3.8 km RHIC tunnel at Brookhaven National Laboratory. It will comprise a Hadron Storage Ring (HSR) for protons/ions up to 275 GeV and a new Electron Storage Ring (ESR) storing electrons at 5, 10, and 18 GeV. The baseline configuration features a single interaction region (IR6), with an upgrade path to a second IR (Fig. 1). The collider will provide center-of-mass energies from approximately 29 to 141 GeV and reach luminosities up to $1 \times 10^{34}\,\mathrm{cm}^{-2}\,\mathrm{s}^{-1}$ with polarized beams (typical average polarization 70 %). During physics stores of $\mathcal{O}(10\,\mathrm{h})$, the electron beam will be operated in continuous "swap-out" injection mode at rates up to 1 Hz to maintain stable current and polarization. The machine parameters used in this study are summarized in Table I.

The ESR collimation insertion is located in IR4 and consists of one primary movable betatron collimator per transverse plane for each energy; its baseline design and implementation are described elsewhere [3].

B. Detector Design

The ePIC detector [6] will be installed at IR6 and comprises low-material silicon vertex/tracking, central tracking and particle identification systems (including Time-of-Flight and Ring-imaging Cherenkov concepts), and electromagnetic and hadronic calorimetry for lepton/photon identification and jet reconstruction. In addition to the central detector, the IR includes auxiliary forward and rear systems (taggers, luminosity monitors, zero-degree calorimeter/roman pots/off-momentum detectors) placed several meters from the IP to extend acceptance to very small angles. Since beam-induced losses near IR6 can generate secondaries and heat load in superconducting elements, accurate loss-map predictions for relevant mechanisms are important for both detector background and machine-protection studies.

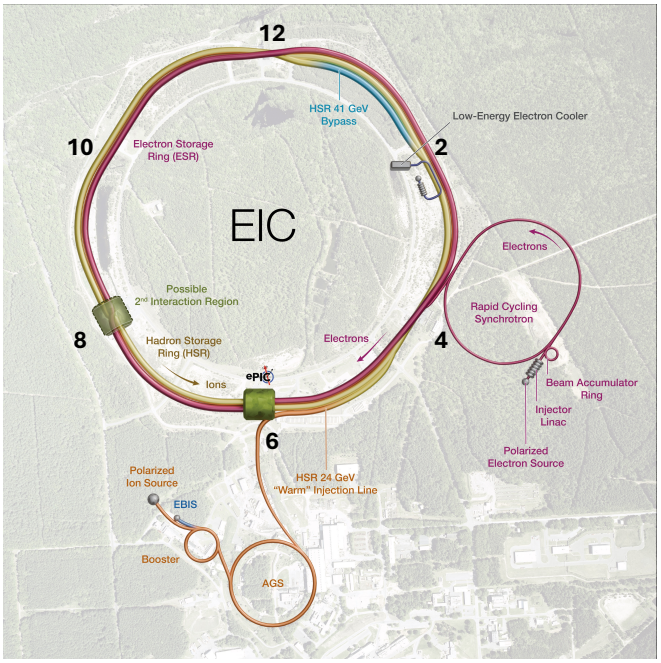

FIG. 1: Schematic drawing of the EIC. The numbers from 2 through 12 indicate six insertion regions around the rings.

III. BEAM LOSS MECHANISMS

Beam losses in the ESR arise from intra-beam scattering, interactions with the residual-gas environment, scattering on thermal-radiation, and hard radiative processes at the IP. These losses can limit beam lifetime, drive localized energy deposition in apertures and superconducting elements near the IR, and generate secondary showers that contribute to detector backgrounds and cryogenic heat load.

Touschek scattering is a hard Coulomb scattering within a bunch that transfers transverse momentum into the longitudinal plane. The resulting momentum offsets can exceed the RF bucket or the ring momentum acceptance, producing losses primarily in dispersive regions and at aperture bottlenecks. In lepton rings, Touschek scattering is often a dominant contributor to lifetime and motivates dedicated collimation.

Beam-gas interactions include elastic Coulomb scattering and inelastic bremsstrahlung on residual-gas molecules. Coulomb scattering increases betatron amplitudes, while bremsstrahlung produces an energy loss. Both mechanisms generate distributed losses around the ring, with patterns shaped by optics, dispersion, and lo-

TABLE I: EIC beam parameters relevant to the studies presented in this work, adapted from Table 3.3 of Ref. [2] and Table 3 (vertex spread) of Ref. [5].

Species	proton	electron	proton	electron	proton	electron
Energy [GeV]	275	18	275	10	100	5
Bunch intensity [10^{10}]	19.1	6.2	6.9	17.2	4.8	17.2
No. of bunches	290		1160		1160	
Beam current [A]	0.69	0.227	1	2.5	1	2.5
RMS emittance, X/Y [nm]	18/1.6	24/2	11.3/1	20/1.3	26/2.3	20/1.8
RMS bunch length [cm]	6	0.9	6	0.7	7	0.7
RMS momentum spread $\Delta p/p$ [10^{-4}]	6.8	10.9	6.8	5.8	9.7	6.8
IP vertex spread, X/Y/Z [mm]	0.243/0.025/37.77		0.206/0.012/36.00		0.189/0.010/32.92	
RMS angular divergence, X/Y [μrad]	206/206	160/160	119/119	211/152	150/150	202/187
Luminosity [10^{33} cm^{-2}s^{-1}]	1.54		10		3.68	

cal apertures.

Bethe-Heitler (BH) bremsstrahlung at the IP, $e^- p \to e^- p \gamma$, produces electrons with large energy loss and/or angle that are typically lost rapidly downstream of the IP. These losses are strongly localized in the IR and can be a significant source of backgrounds for near- and far-forward instrumentation, motivating dedicated loss-map and shielding studies.

Thermal-radiation (blackbody) Compton scattering is the scattering of stored electrons on thermal photons emitted by the warm vacuum chamber. While typical photon energies at 300 K are $\mathcal{O}(0.1\,\mathrm{eV})$, the large Lorentz boost makes rare events with sizable electron momentum deviation possible; these can contribute to distributed losses and lifetime reduction, especially at higher electron energy and low residual-gas pressure. In this work, thermal Compton scattering is modeled with a KN-correct Monte Carlo generator and compared to the above mechanisms using loss maps, loss timing distributions, and lifetime estimates.

IV. THERMAL COMPTON SCATTERING MODEL

A. Thermal Photon Field

We model the vacuum chamber as a blackbody photon field at temperature $T = 300\,\mathrm{K}$. The blackbody photon number density is [1]: $n_{\mathrm{ph}}[\mathrm{cm}^{-3}] = 20.2\,T^3$. For $T = 300\,\mathrm{K}$, $n_{\mathrm{ph}} \approx 5.45 \times 10^8\,\mathrm{cm}^{-3}$, and the average photon energy is $\langle\omega\rangle = 2.7\,k_{\mathrm{B}}T \approx 0.07\,\mathrm{eV}$.

B. Compton vs Thomson and the Klein-Nishina spectrum

In the electron rest frame (ERF, S^*), Compton scattering is described by the KN differential cross section. In the limit of small incident photon energy, $k^* \ll m_{\mathrm{e}}c^2$, the angular dependence approaches the Thomson form, $d\sigma_{\mathrm{T}}/d\Omega \propto 1 + \cos^2\theta$, with total cross section $\sigma_{\mathrm{T}} = 6.65 \times 10^{-25}\,\mathrm{cm}^2 = 665\,\mathrm{mb}$.

In our Monte Carlo generator, we use the Thomson distribution as a proposal and recover the KN result via event-by-event acceptance based on the ratio $(d\sigma_{\mathrm{KN}}/d\Omega)/(d\sigma_{\mathrm{T}}/d\Omega)$, following the algorithmic strategy described in Ref. [4].

We adopt the same coordinate conventions as used in the analytic kinematics treatment of inverse Compton scattering in Ref. [7]: in the laboratory frame S the incoming electron defines the $+z$ axis; a thermal photon is sampled isotropically in S and boosted into the ERF S^*; in S^* we rotate so that the incoming photon momentum is aligned with $+z$, sample the scattering angles (θ, ϕ) with respect to this axis, then rotate back and boost the scattered photon to S. The scattered-electron four-momentum is obtained from energy-momentum conservation, consistent with the modular boost/rotation approach emphasized by H. Burkhardt [4].

For the EIC ESR, thermal photon energies are tiny in the lab frame, but boosts into the ERF and rare-angle kinematics necessitate the full Compton (Klein-Nishina) treatment to obtain correct tails and energy shifts.

C. Event Generation Algorithm

We implement the Monte Carlo approach as described in Ref. [4], adapted for embedding into multi-turn tracking at the EIC. We generate thermal Compton events by sampling a thermal photon in the laboratory frame and performing the scattering in the ERF. For each trial, the following steps are executed:

1. **Incoming electron in the laboratory frame.** The incoming electron 4-vector $P_{\mathrm{e}} = (E_{\mathrm{e}}, \mathbf{p}_{\mathrm{e}})$ is constructed from the tracking variables $(x, y, z, x', y', \delta)$. The electron velocity used for boosts is $\beta_{\mathrm{e}} = |\boldsymbol{p}_{\mathrm{e}}|/E_{\mathrm{e}}$ (with $c = 1$).

2. **Thermal photon sampling in the laboratory frame.** The incoming photon energy k is sampled from the blackbody photon-number spectrum at temperature T, and the photon direction is sampled isotropically. The photon four-vector is $P_\gamma = (k, \mathbf{k})$ with $|\mathbf{k}| = k$.

3. **Boost to the ERF.** The photon four-vector is Lorentz-boosted from the laboratory frame to the ERF using β_e, yielding $(k^*, \mathbf{k}^*)$.

4. **ERF rotation for angular sampling.** A rotation matrix R is constructed such that $R\hat{\mathbf{k}}^* = \hat{\mathbf{z}}$. Rather than explicitly rotating the incoming photon, we use this rotation to define a local coordinate system in which the scattered photon is first constructed with respect to the $\hat{\mathbf{z}}$ axis (i.e., in the "rotated ERF frame") and is then rotated back to the original ERF orientation using R^{T}.

5. **Thomson-angle proposal.** A single candidate scattering direction (θ, ϕ) is proposed from the Thomson angular distribution: $d\sigma_{\mathrm{T}}/d\Omega \propto 1 + \cos^2\theta$, using an exact sampler.

6. **Klein-Nishina acceptance and Compton energy shift.** The proposed trial is accepted with probability

$$\mathcal{R}(\theta, k^*) = \frac{(d\sigma_{\mathrm{KN}}/d\Omega)}{(d\sigma_{\mathrm{T}}/d\Omega)}$$

evaluated in the ERF at (k^*, θ). If accepted, the scattered photon energy in the ERF is computed via the Compton relation

$$x \equiv \frac{k^*_{\mathrm{out}}}{k^*_{\mathrm{in}}} = \frac{1}{1 + \frac{k^*_{\mathrm{in}}}{m_e}(1 - \cos\theta)},\ k^*_{\mathrm{out}} = x k^*_{\mathrm{in}}\,.$$

The outgoing photon momentum is constructed in the rotated ERF frame as

$$k^*_{\mathrm{out,rot}} = k^*_{\mathrm{out}}(\sin\theta\cos\phi, \sin\theta\sin\phi, \cos\theta)\,,$$

then rotated back as $\boldsymbol{k}^*_{\mathrm{out}} = R^{\mathrm{T}}\boldsymbol{k}^*_{\mathrm{out,rot}}$.

7. **Boost back to the laboratory frame and electron reconstruction.** The scattered photon is boosted back to the laboratory frame using β_e. The outgoing electron four-vector is obtained by four-momentum conservation in the laboratory frame:

$$P_{\mathrm{e,out}} = P_{\mathrm{e,in}} + P_{\gamma,\mathrm{in}} - P_{\gamma,\mathrm{out}}\,.$$

This procedure uses a Thomson proposal with a single-shot KN acceptance/rejection per trial, producing accepted events distributed according to the KN differential cross section while retaining a convenient normalization based on σ_{T}.

D. Photon Energy Sampling

The photon energies are sampled from the blackbody photon-number distribution:

$$p(E)dE \propto E^2/(\exp(E/kT) - 1)dE\,.$$

We use the identity:

$$\frac{1}{e^x - 1} = \sum_{n=1}^{\infty} e^{-nx}\,,$$

with $x = E/(kT)$, which turns the distribution into a mixture of Gamma distributions:

- choose n with probability $\propto 1/n^3$,
- sample $x \sim \mathrm{Gam}(3, 1/n)$,
- return $E = x \cdot kT$.

A truncation $n \le n_{\max}$ is used (default 2000 in the implementation) and is sufficient for 300 K tails in this application.

E. Output Kinematics

To interface with tracking codes, the scattered electron and photon are returned in a 6D-like form: $(x, y, z, x', y', \delta)$, where $x' = p_x/p_z$, $y' = p_y/p_z$, and $\delta = (p/p_0) - 1$, with p_0 computed from a reference beam energy E_b as $p_0 = \sqrt{E_b^2 - m_e^2}$. Events with $p_z \le 0$ are rejected (or flagged) to preserve forward-motion conventions in the ring coordinate system.

F. Absolute Rate Normalization

A central goal is to assign each accepted event an absolute rate weight (Hz) so that summing weights yields the physical scattering (or loss) rate. The beam current corresponds to an electron flow rate through a point: $\dot{N} = I/e$.

For photon number density $\rho_\gamma(T)$ [$1/\mathrm{m}^3$] and cross section σ, the interaction probability per unit length is $\rho_\gamma\sigma$, so a section of length L has collision rate: $R = (I/e)\rho_\gamma\sigma L$.

In our method, we use σ_{T} as a trial cross section and accept candidates with probability $\mathcal{R}(\theta, k^*)$. For a macro-ensemble of N_{macro} particles/electrons and K trials per macro per section call, each trial represents an effective path length L/K, and each accepted trial receives weight: w_{trial} [Hz] $= (I/(eN_{\mathrm{macro}}))\rho_\gamma(T)\sigma_{\mathrm{T}}(L/K)$.

Summing w_{trial} over accepted events yields the Compton collision rate for that section; summing w_{trial} only over events whose scattered electron is lost yields the loss rate.

G. Tail Selection

To control computational cost and focus on loss-relevant tails, we keep only scattered electrons with $|\delta| \ge \delta_{\mathrm{threshold}} = 10^{-3}$ for tracking. This is a numerical/importance threshold and is significantly smaller

than the ESR momentum acceptance ($> 5 \times 10^{-3}$) [3]. The threshold ensures that (i) rare but loss-relevant energy deviations are captured, while (ii) extremely small-angle, tiny-δ scatters that do not affect lifetime are not unnecessarily tracked.

V. MULTI-TURN TRACKING INTEGRATION AND SIMULATION ASSUMPTIONS

A. Tracking Workflow Overview

Thermal Compton scattering is incorporated into the multi-turn tracking framework described in Ref. [3] by applying the event generator independently in each ring section. For each section,

- the stored beam is represented by a set of 6D macro-electrons $(x, y, z, x', y', \delta)$,
- blackbody photons are sampled at $T = 300\,\mathrm{K}$,
- Compton events are generated with the algorithm described above, including absolute rate weights, and
- the scattered particles are tracked through the lattice with the aperture/collimator model until they are lost or the tracking turn limit is reached.

For comparison, we use Monte Carlo samples of scattered electrons from beam-gas interactions (Coulomb and bremsstrahlung) and Touschek scattering from the study documented in Ref. [3].

Bethe-Heitler bremsstrahlung losses at the interaction point are modeled using the following workflow:

- impose a minimum electron energy loss of 1 MeV (Step 1),
- compute BH cross sections with the GETaLM framework [8] (Step 2),
- compute the total BH scattering rate at the IP using the luminosity from Table I (Step 3),
- generate scattered-electron samples at the IP including beam effects and realistic vertex distributions in GETaLM (Step 4), and
- select a representative subset, assign weights, and track through the lattice to obtain loss maps and lifetimes (Step 5).

The resulting BH cross sections at 5, 10, and 18 GeV are 467, 559, and 624 mb, corresponding to total electron loss rates of approximately 1.73, 5.59, and 0.94 GHz, respectively. This procedure defines the BH normalization directly from the IP scattering rate and enables a consistent comparison to the other loss mechanisms considered in this work.

The same ring aperture and collimator model is included in all tracking studies. For the configuration used here, the primary collimators are modeled with a tungsten head length of 5 cm and are set to the optimal apertures reported in Ref. [3].

With synchrotron radiation and RF enabled, we tracked approximately 2×10^8 scattered macro-particles for the combined beam-gas and Touschek sample, 3×10^6 for thermal-radiation scattering, and 1×10^7 for the BH sample. The lattice model (v6.3.1) does not include machine errors such as element misalignments or magnetic field errors.

VI. RESULTS: LOSS MAPS, TIMING, AND LIFETIMES

A. Ring Loss Maps and Lifetimes

Figure 2 shows the ESR loss map and the corresponding beam lifetimes for thermal-radiation scattering, together with the Bethe-Heitler (BH) and beam-gas+Touschek reference results. For the configuration studied here, the shortest lifetime is set by beam-gas+Touschek at 5 GeV ($\sim 3\,\mathrm{h}$) and at 10 GeV ($\sim 9\,\mathrm{h}$), while at 18 GeV the limiting contribution is BH ($\sim 14\,\mathrm{h}$).

The thermal-radiation lifetimes obtained for the three energies (100-700 h) are consistent with the analytic estimates of V. Telnov; see Fig. 3 (5 and 15 GeV curves) in Ref. [1].

At sufficiently low luminosity (e.g., $\sim 1 \times 10^{32}\,\mathrm{cm^2\,s^{-1}}$), thermal-radiation scattering can become the dominant lifetime limitation, since the BH loss rate scales linearly with luminosity. In the EIC swap-out injection mode, however, beam lifetimes of a few to $\mathcal{O}(10)$ hours do not constrain operations, because individual electron bunches are continuously replaced at rates up to 1 Hz.

A key qualitative observation is that thermal-radiation scattering generates losses distributed around the ring, whereas BH losses are more strongly localized near IR6. In addition, at 18 GeV both BH and thermal-radiation loss rates at the IR4 collimators can exceed those from the beam–gas+Touschek reference in the same configuration.

B. Loss Timing Distributions

Figure 3 shows loss timing ("turn when lost"). All mechanisms are multi-turn with large first-turn losses and a long tail, and their timing is broadly similar in the studied setup.

For thermal-radiation specifically, tracking beyond 100 turns is computationally expensive and yields little additional contribution to loss-rate estimates because the per-turn loss rate drops by orders of magnitude after ~ 100 turns.

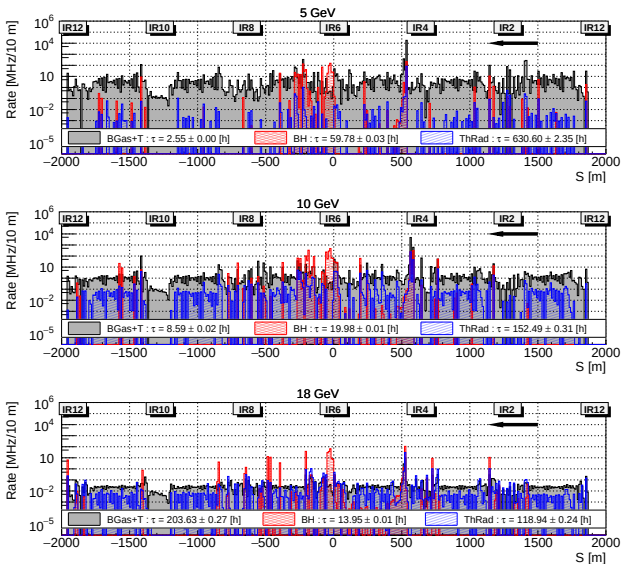

FIG. 2: ESR loss map and corresponding beam lifetime. The electron beam direction is indicated by the arrow. The collimation insertion is located in IR4, where the highest loss rates are expected. "BGas+T", "BH", and "ThRad" refer to beam-gas+Touschek, Bethe-Heitler bremsstrahlung, and thermal-radiation losses, respectively.

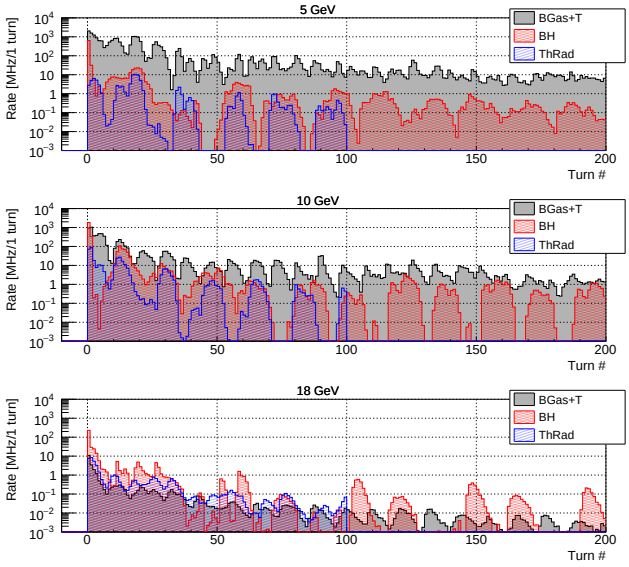

FIG. 3: Loss timing distribution (i.e., turn number when lost).

C. Interaction Region Losses

In IR6 (Fig. 4), BH losses are predominantly localized downstream of IP6 and occur at a higher rate than the beam-gas+Touschek reference, indicating that BH losses should be included in ePIC background studies. BH losses upstream of IP6 with large momentum deviation follow the Touschek-like loss pattern [3], whereas BH losses dominated by large angular deviations are more consistent with beam-gas loss distributions. As expected, the highest BH loss rate occurs in the region downstream of the electron dipole (5 m long, 20 mrad bend, located ~ 20 m downstream of the IP), extending into the auxiliary detector section ($25 - 40$ m downstream of the IP). These losses are therefore expected to be the dominant background source for the taggers.

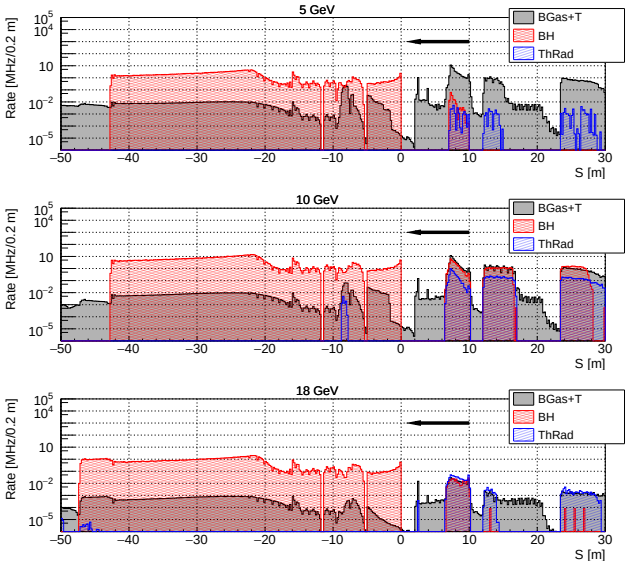

FIG. 4: IR6 beam losses. The ePIC detector region expends to 5 m from the IP ($S = 0$ m) on both sides. The electron beam direction is indicated by the arrow.

Thermal-radiation losses in IR6 are predominantly localized in the forward cryostat ($S > 5$ m), with a rate comparable to beam-gas+Touschek, and with almost no losses in the immediate ePIC region (± 5 m from the IP) for the configuration studied here. The thermal-radiation loss pattern closely follows the Touschek loss distribution.

The study also suggests that the BH heat load ($100 - 1000$ mW) is approximately an order of magnitude higher than that from beam-gas+Touschek (< 200 mW), while the thermal-radiation heat load (< 20 mW) is lower than both but may still contribute to localized heating. Consequently, both BH and thermal-radiation components should be included in IR6 cryostat heat-load assessments, although synchrotron radiation power ($\mathcal{O}(1\,\mathrm{kW})$) is expected to dominate the overall budget. A dedicated IR6 heat-load analysis is beyond the scope of this paper and will be addressed in future work.

VII. VALIDATION, REPRODUCIBILITY, AND PUBLIC SOFTWARE RELEASE

A. Validation Strategy

Because the goal is public dissemination of a working and reusable scattering routine, we include validation scripts that do not require access to the project-specific tracking workflow. The validation suite includes:

A) Photon sampler validation ($T = 300\,\mathrm{K}$): sampled energy histogram compared to analytic shape $E^2/(\exp(E/kT)-1)$; check mean energy $\sim 2.7 k_\mathrm{B}T$ ($\approx 0.07\,\mathrm{eV}$ at $300\,\mathrm{K}$); see Fig. 5.

B) Thomson angular sampler: verify $\cos\theta$ distribution proportional to $(1+\cos^2\theta)$ and ϕ uniform; see Fig. 6.

C) KN acceptance: verify accepted $\cos\theta$ and ERF energy shift x reproduce KN predictions for representative k^*; see Fig. 7.

D) Kinematics consistency: check photon masslessness ($E^2 - |p|^2 \approx 0$), electron mass shell, and 4-momentum conservation.

E) Absolute rate checks: verify that total event rate scales linearly with beam current I and path length L, and scales as T^3 via photon density; verify agreement with rough minimum-lifetime estimate $\tau_\mathrm{min} \approx 1/(n_\mathrm{ph}\sigma_\mathrm{T}cf) \approx 24\,\mathrm{h}$ under the extreme assumption that all scattered particles are lost ($f = 1$).

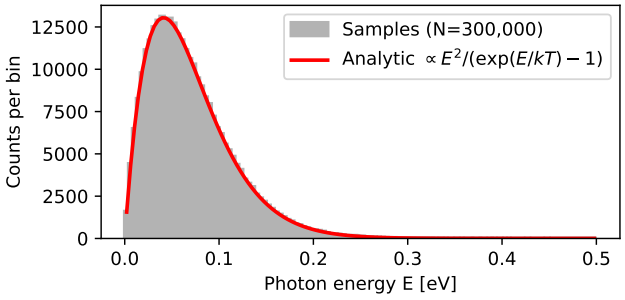

FIG. 5: Photon-energy sampler validation at $T = 300\,\mathrm{K}$. Histogram of sampled blackbody photon energies (photon-number spectrum) compared to the analytic shape, normalized over the plotted range.

We emphasize this is a cross-check; actual lifetime depends on machine acceptance and the fraction of scatters that exceed it.

B. Public repository contents

The public release [9] includes the ThermalCompton class (PYTHON) implementing the event generator,

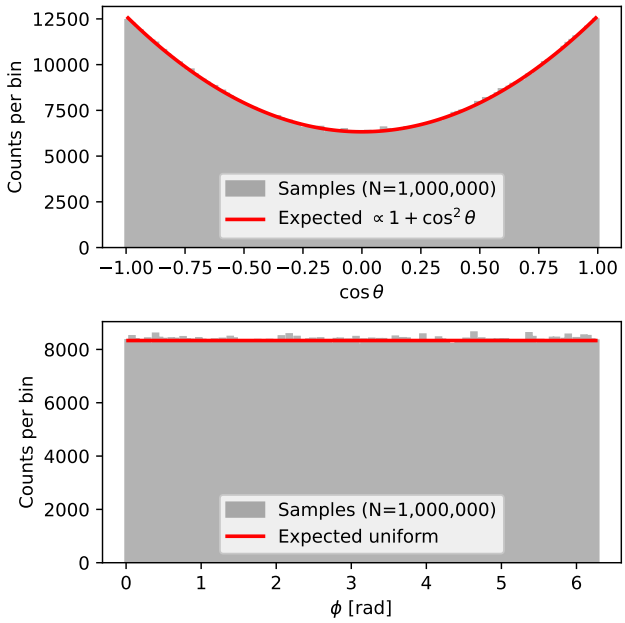

FIG. 6: Validation of the Thomson angular sampler. Top: sampled $\cos\theta$ distribution compared to the expected Thomson shape $d\sigma_\mathrm{T}/d\Omega \propto 1+\cos^2\theta$. Bottom: sampled azimuthal angle ϕ distribution compared to a uniform distribution on $[0, 2\pi)$.

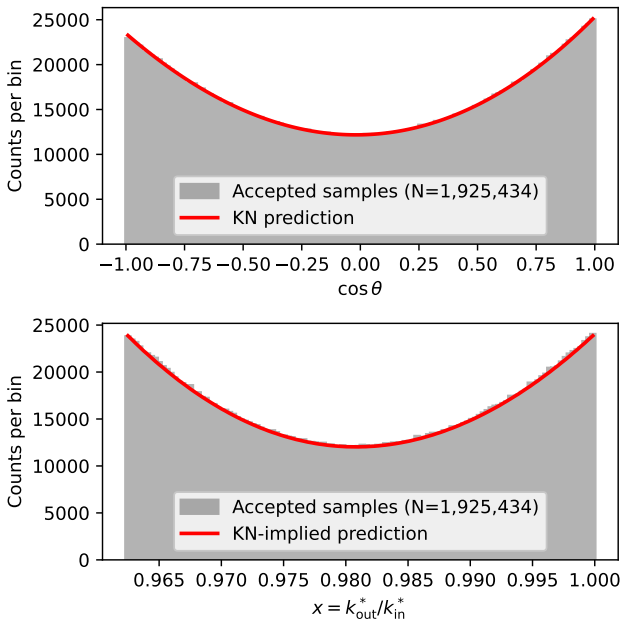

FIG. 7: Validation of the KN acceptance procedure for a fixed representative ERF photon energy k^*. Top: distribution of accepted $\cos\theta$ compared to the KN prediction. Bottom: distribution of the ERF energy shift $x = k^*_\mathrm{out}/k^*_\mathrm{in}$ for accepted events compared to the KN-implied expectation obtained from the same angular distribution.

minimal driver scripts to generate events without a lattice and reproduce validation plots, example interfaces to a generic tracking code, and documentation describing required inputs (beam energy, current, temperature, trials, δ threshold) and output conventions.

VIII. DISCUSSION AND LIMITATIONS

The thermal photon field is modeled as isotropic blackbody at uniform temperature $T = 300\,\mathrm{K}$. Extensions could include non-uniform temperature or localized warm components.

The δ threshold used for computational efficiency ($|\delta| \geq 10^{-3}$) is well below the ESR momentum acceptance and is not itself a physics acceptance cut; it is a numerical filtering threshold used to focus on potentially relevant tails [3].

The ring and IR loss maps depend on the lattice/aperture/collimator model used in tracking; the presented loss-map results are specific to the studied configuration and should be updated as the ESR design evolves.

For BH losses, the normalization depends on GETaLM cross sections and the assumed luminosity; systematic studies of uncertainties (cross sections, vertex distributions, and beam effects) will be revisited as the EIC design matures.

IX. CONCLUSIONS

We presented a standalone, publicly-released Monte Carlo event generator for thermal Compton scattering of stored electrons on blackbody photons, designed for integration into multi-turn tracking workflows and for public release with reproducible validation tests. The generator uses Thomson-angle proposal sampling with Klein-Nishina rejection following H. Burkhardt, samples photon energies from the blackbody photon-number distribution using a mixture method, and assigns each event an absolute rate weight (Hz) consistent with beam current and photon density. Embedded into the EIC ESR tracking workflow, the model predicts that thermal-radiation can produce distributed losses around the ring and localized IR6 losses predominantly in the forward cryostat, with minimal losses in the immediate ePIC region for the studied case. The estimated thermal-radiation beam lifetimes agree well with V. Telnov calculations.

At 18 GeV, thermal-radiation yields a lifetime ($\sim$ 120 h) shorter than beam-gas+Touschek ($\sim$ 200 h) but longer than Bethe-Heitler bremsstrahlung ($\sim$ 14 h) in the studied configuration.

These results motivate including thermal-radiation scattering (alongside BH) in high-energy ESR lifetime, loss-map, and IR protection/heat-load assessments.

ACKNOWLEDGMENTS

We thank our colleagues in the EIC Project and the ePIC Collaboration for valuable discussions and for sharing key technical information on the interaction region and detector configuration used in this study. We also acknowledge the Jefferson Lab Scientific Computing Team for access to the JLab computing farm, which supported the large-scale, CPU-intensive simulations required for this work.

This work was supported by the U.S. Department of Energy under contract number DE-SC0012704.

[1] V. Telnov, Scattering of electrons on thermal radiation photons in electron-positron storage rings, Nucl. Instrum. Methods Phys. Res. 260 (2) (1987) 304–308. doi:https://doi.org/10.1016/0168-9002(87)90093-3.
URL https://www.sciencedirect.com/science/article/pii/0168900287900933

[2] F. Willeke and J. Beebe-Wang, Electron Ion Collider Conceptual Design Report 2021, Tech. rep., BNL-221006-2021-FORE; TRN: US2215154 (2021). doi:10.2172/1765663.

[3] A. Natochii *et al.*, A Collimation System Baseline Design for the Electron Storage Ring at the Electron-Ion Collider (2025). arXiv:2512.19502.
URL https://arxiv.org/abs/2512.19502

[4] H. Burkhardt, Monte Carlo simulation of scattering of beam particles and thermal photons, Tech. rep., CERN, Geneva (1993).
URL https://cds.cern.ch/record/703373

[5] J. Adam *et al.*, Accelerator and beam conditions critical for physics and detector simulations for the Electron-Ion Collider (Jul. 2021). doi:10.5281/zenodo.6514605.
URL https://zenodo.org/records/6514605

[6] ePIC Collaboration, The ePIC Detector, https://www.epic-eic.org/public/detector.html, accessed: 2026-02-18.

[7] A. Di Domenico, Inverse Compton Scattering of Thermal Radiation at LEP and LEP-200, Particle Accelerators 39 (1992) 137–146.
URL https://s3.cern.ch/inspire-prod-files-1/112d07f6d60840037a97affa44c6718e

[8] J. Adam, GETaLM: A generator for electron tagger and luminosity monitor for electron - proton and ion collisions, Comput. Phys. Commun. 272 (2022) 108251. doi:https://doi.org/10.1016/j.cpc.2021.108251.
URL https://www.sciencedirect.com/science/article/pii/S0010465521003635

[9] A. Natochii, Thermal Compton Monte Carlo event generator, https://github.com/eic/thermal-compton-mc, accessed: 2026-02-20 (2026).